ChemComm

Check for updates

Advances in electrically driven light-emitting diodes based on lead-free metal halides

Shu-Hua Xue,[ab] Jia-Yu Yao,[a] Liang-Jin Xu ⓘD *[abcd] and Zhong-Ning Chen ⓘD [abcd]

The emerging lead halide perovskites show great potential for their use as emitters in electrically driven light-emitting diodes (LEDs) with external quantum efficiency (EQE) over 25%. While the toxicity of lead and inferior device stability are the main obstacles for their commercialization, replacing Pb^{2+} with low- or non-toxic metal ions to form low- or zero-dimensional structures provides an alternative approach to effectively tackle these issues. Recently, luminescent lead-free metal halides have been increasingly developed toward eco-friendly and highly efficient electroluminescence. In this feature article, we give a brief overview of recent advances in luminescent lead-free metal halides and their applications in electrically driven LEDs. The challenges and prospects in this field are outlined at the end.

1. Introduction

Organic light-emitting diodes (OLEDs) have been commercially used in flat-panel displays and lighting.[1,2] Light-emitting materials play a critical role in achieving highly efficient OLEDs.[3–6] Green and red phosphors based on iridium(III) complexes have been employed in commercialized OLEDs due to their excellent stability, tunable emission and superior device efficiency.[7]

[a] State Key Laboratory of Structural Chemistry, Fujian Institute of Research on the Structure of Matter, Chinese Academy of Sciences, Fuzhou 350002, China.
E-mail: xuliangjin@fjirsm.ac.cn
[b] College of Chemistry and Material Science, Fujian Normal University, Fuzhou 350007, China
[c] Fujian Science & Technology Innovation Laboratory for Optoelectronic Information of China, Fuzhou 350108, China
[d] University of Chinese Academy of Sciences, Beijing 100039, China

However, the low abundance of iridium on the earth is not conducive to its sustainable development.[8] Recently, lead(II) based perovskites as a class of rising star materials for optoelectronic devices show great potential for their use in electrically driven LEDs,[9,10] owing to their tunable emission colors, high quantum yield (PLQY) and narrow-band emission. Substantial progress has been made in perovskite-based light-emitting devices (PeLEDs) with EQE exceeding 25% for both green and red emissions.[11,12] Despite their superior performance in terms of EQE, current efficiency, brightness, emission color and color purity, the commercial deployment of PeLEDs is extremely hindered by a number of challenges, such as a great drop in EQE at elevated current densities, the intrinsic toxicity of lead and instability of devices.[13]

To surmount the issues faced in 3D lead perovskites, several feasible strategies have been proposed.[14,15] Among them,

Shu-Hua Xue is an academic master candidate at Fujian Normal University. She received her bachelor's degree from Qingdao University in 2021. Her research mainly aims at the preparation of organic–inorganic halide hybrids and their applications in optoelectronics.

Shu-Hua Xue

Jia-Yu Yao is an academic master candidate at Fuzhou University. She received her bachelor's degree from Yangtze University in 2022. Her research mainly aims at the preparation of organic–inorganic halide hybrids and their applications in optoelectronics.

Jia-Yu Yao

Table 1 Summary of electrically driven LEDs based on lead-free metal halides

Metal halides LEDs	Emission layer	Luminance (cd m^{-2})	PLQY (%)	EQE (%)	EL (nm)	FWHM^a (nm)	Year/Ref.
Sn-based LEDs	CsSnI$_3$	—	—	3.8	950	—	2016[33]
	CsSnI$_3$	—	—	5.4	945	—	2021[34]
	CH$_3$NH$_3$SnI$_3$	—	30	5.3	866	—	2022[27]
	PEA$_2$SnI$_4$	0.15	—	—	618	—	2017[19]
	PEA$_2$SnI$_4$	70	1.4	0.3	633	24	2020[26]
	PEA$_2$SnI$_4$	20	7	5	632	21	2020[18]
	(PEAI)$_x$(CsI)$_y$(SnI$_2$)	—	18	3	920	—	2019[28]
	CsSnBr$_3$	160	1.47	—	674	—	2022[29]
	TEA$_2$SnI$_4$	322	1.52	0.62	638	28	2020[31]
	(BTm)$_2$SnI$_4$	3466	7.5	3.33	653	27.8	2022[32]
Cu-based LEDs	Cs$_3$Cu$_2$I$_5$	10	62.1	—	445	—	2021[30]
	Cs$_3$Cu$_2$I$_5$	262.6	87	1.12	445	63	2018[36]
	Cs$_3$Cu$_2$I$_5$	70	58	0.1	440	70	2020[38]
	Cs$_3$Cu$_2$I$_5$	—	96.6	—	460	—	2020[37]
	CsCu$_2$I$_3$	47.5	20.6	0.17	550	100	2022[39]
	CsCu$_2$I$_3$	100	84.8	7.4	568	132	2020[41]
	CsCu$_2$I$_3$	10	21.4	0.02	560	180	2021[45]
	Cs$_3$Cu$_2$I$_5$: CsCu$_2$I$_3$	1570	30	3.1	565	121	2020[44]
	1D-Cu$_4$I$_6$(bttmp)$_2$	642.4	91	5.02	562	123	2021[48]
Mn-based LEDs	[PPh$_4$]$_2$[MnBr$_4$]	2339	—	9.6	518	—	2021[46]
	DBFDPO-MnBr$_2$	10.5	81.4	10.5	548	—	2017[20]
	(C$_{39}$H$_{35}$P$_2$) MnBr$_4$	24.7	48	7.12	516	45	2019[50]
	(ABI)$_4$MnBr$_6$	4700	80	9.8	627	45	2021[51]
Sb-based LEDs	Cs$_3$Sb$_2$I$_9$	—	—	10^{-8}	780	—	2021[52]
	Cs$_3$Sb$_2$Br$_9$	29.4	—	0.21	408	—	2019[53]
	(MePPh$_3$)$_2$SbCl$_5$	3500	99.4	3.1	593	110	2020[54]
Ln-based LEDs	Cs$_3$CeBr$_6$	—	91	—	391/421	0.5	2022[55]
	CsEuBr$_3$	—	69	—	448	6.5	2021[56]

^{a} Full width at half maximum.

replacing Pb^{2+} with low- or non-toxic metal ions to form perovskite-related materials effectively alleviates the toxicity issues. Using appropriate combinations of large organic cations and non-lead metal halides to form low-dimensional metal halide hybrids improves dramatically the stability.[16,17] To this end, great efforts have been made to develop eco-friendly light-emitting materials for achieving electrically driven LEDs in recent years. For example, Sargent *et al.* reported a bunch of Sn-based 3D perovskite LEDs with EQE higher than 5%.[18] Hauqe's group first demonstrated that the 2D tin hybrids could act as emitting layers for achieving efficiently electro-driven LEDs.[19] In 2017, our group conducted a pioneering work on electrically driven LEDs based on 0D lead-free metal halide hybrids by using [PPh$_4$]$_2$[MnBr$_4$] (PPh$_4^+$ = tetraphenyl phosphonium) as a green emitter.[20] Thereafter, more and more lead-free metal halides have been developed toward achieving highly efficient electro-driven LEDs as summarized in Table 1.

To date, several reviews have discussed the research progress of metal halides as light-emitting materials,[21,22] involving the synthesis strategy for lead-free materials and their luminescence mechanisms along with their great development potential in the field of down-conversion LEDs.[23,24] Nevertheless,

Liang-Jin Xu

Liang-Jin Xu is currently a professor in Fujian Institute of Research on the Structure of Matter, Chinese Academy of Sciences. He obtained his bachelor's degree from Central China Normal University in 2010 and PhD degree from Fujian Institute of Research on the Structure of Matter, Chinese Academy of Sciences. His research interests are luminescent organic–inorganic hybrids, phosphorescent metal complexes and their application in opto-electronic devices such as OLEDs, Scintillators, and Sensors.

Zhong-Ning Chen

Zhong-Ning Chen received his PhD in Chemistry from Nanjing University in 1994. Since 2001, he has been a professor in Fujian Institute of Research on the Structure of Matter, Chinese Academy of Sciences. His research fields are coordination chemistry and organometallic chemistry, focusing on non-iridium phosphorescent materials and devices, organometallic wires, and metal-coordination switches and sensors.

electrically driven LEDs based on lead-free metal halides have not been reviewed as a single topic. In this article, we review the recent advances in electrically driven LEDs based on Pb-free metal halides as light-emitting materials, focusing on innovative device performance and preparation methods. A brief conclusion and perspective on future challenges and opportunities of electrically driven LEDs based on lead-free metal halides are presented in the last section. Although the focus of this paper is mainly lead-free metal halide materials, we believe that the contents and insights of this study are also applicable to the relevant fields of metal halides for emerging optoelectronic applications.

2. Sn(II)-based electrically driven LEDs

Light-emitting diodes based on 3D lead(II) halide perovskites have been demonstrated to provide superior external quantum efficiency and tunable emissions covering from blue to near-infrared light. However, the issues of intrinsic toxicity and instability of lead(II)-based 3D perovskites need to be addressed before further commercial applications.[25] An available approach to effectively surmount the issues of toxicity and stability is replacing Pb^{2+} with low- or non-toxic metal ions to form low- to zero-dimensional structures. Therefore, much effort has been made to develop LEDs based on eco-friendly metal halide materials.

Among the developed lead-free metal halides, tin-based halides have attracted much attention in recent years due to their properties similar to those of lead-based perovskites such as a narrow-band gap (1.2–1.4 eV), a high carrier mobility (102–103 cm^2 $V^{-1}s^{-1}$) and low exciton binding energy. Thus, tin halides show great potential to be used as light-emitting materials for achieving highly efficient and eco-friendly LEDs. Easy oxidation of Sn^{2+} to Sn^{4+}, low formation energy of tin vacancies, heterogeneous nucleation and crystal growth rates are the main obstacles for attaining highly efficient LEDs. Several strategies have been proposed to overcome these obstacles. Sargent et al. used H_3PO_2 to prevent the oxidation of Sn^{2+} and promote crystal growth during film formation.[26] In addition to H_3PO_2, sodium salt of 2,3-dihydroxynaph-thalene-6-sulfonic acid (DSAS), valeric acid (VA), and Eu^{3+} ions can also be used as antioxidant additives to prevent Sn^{2+} oxidation. They developed a strategy to improve film quality and protect Sn^{2+} from oxidation through the addition of VA, and the as-fabricated PEA_2SnI_4 LEDs exhibited an EQE of 5% and an operating half-life over 15 hours[18] as illustrated in Fig. 1b.

Wang and his colleagues chose another antioxidant additive PH (PH = phenylhydrazine hydrochloride) to avoid oxidation. A vapor-assisted spin-coating method was used during the recrystallization process, which could improve the crystalline quality of tin perovskites significantly and the film preparation procedure is shown in Fig. 1a.[27] In addition to the easy oxidation of Sn^{2+}, Sn-based LEDs also have an inferior film morphology, which leads to poor device stability and reproducibility. Therefore, they reported a simple and convenient method using

Quasi-2D $(PEAI)_x(CsI)_y(SnI_2)_z$ perovskite multiple quantum wells (MQWs) to achieve efficient and stable lead-free LEDs. The structure of the MQWs is shown in Fig. 1d. Uniform tin-based halides films were realized by partially replacing the Cs^+ cations of 3D $CsSnI_3$ perovskite with bulky PEA cations. The MQW based LEDs exhibit a high radiance of 40 W Sr^{-1} m^{-2} and a peak EQE of 3% (Fig. 1c).[28]

Later, Tan's group prepared PEA_2SnI_4 thin films by using toluene as the antisolvent. They found that replacing the PEAI spacer cation with 2-thiopheneethylamine iodide (TEAI) could give a better device performance. The as-fabricated devices based on TEA_2SnI_4 had a low turn-on voltage of 2.3 V, a maximum luminance of 322 cd m^{-2} and an EQE of 0.62%.[31] The rapid crystallization of Sn^{2+} leads to a poor perovskite morphology with a high trap state, which is also a factor affecting the efficiency of Sn-based LEDs that cannot be ignored. Subsequently, researchers further improved the luminous efficiency and stability of tin-based LEDs by controlling the crystallization of $CsSnBr_3$ in the film forming process. The brightness of the device without additives can be increased by 7500 times, and the device lifetime can be increased to ca. 30 h at 58 cd m^{-2} (Fig. 1e and f).[29] Notably, the emission range of Sn-based LEDs can reach the near-infrared emission region (>810 nm), which is beyond the range of PeLEDs of lead(II) halides. Dou et al. found that Sn(II) based organic perovskite hybrid quantum wells (HQWs) could enhance charge transport and greatly inhibit ion migration by adding an organic barrier with a small band gap to the HQWs (HQW configuration in Fig. 1g). A pure red emitting device was fabricated based on this material with the maximum brightness of 3466 cd m^{-2}, the peak EQE of 3.33%, and operation stability over 150 hours (Fig. 1h).[30] Wei et al. reported near-infrared PeLEDs based on 3D $CsSnI_3$ with an EQE of 5.4%, higher than the one based on $CsSnI_3$ reported by Chao's group in 2016 with an EQE of 3.8%.[32] More importantly, the dendritic structure shows great advantages in flexible devices. After 50 times of bending, the device still maintained 93.4% of the initial EQE.[33]

3. Cu(I)-based electrically driven LEDs

Copper(I) halide based materials have attracted great attention in recent years due to their structural diversity and unique optical properties along with low toxicity, and demonstrate strong potential for general lighting-related applications. Several types of structures with different inorganic building motifs have been developed.[34] Among them, $Cs_3Cu_2I_5$ with a zero-dimensional crystal structure and $CsCu_2I_3$ with a one-dimensional chain structure have been intensively investigated. Besides, copper(I) halide-based inorganic–organic hybrids with strong Cu–N coordination bonds are also promising candidate materials for electrically driven LEDs. Jun et al. found that $Cs_3Cu_2I_5$ exhibited a 0D structure with blue emission (≈ 445 nm), which has a high PLQY of 90% and good air stability. The blue LED device was obtained by using the film prepared through the solution process. Fig. 2a shows a
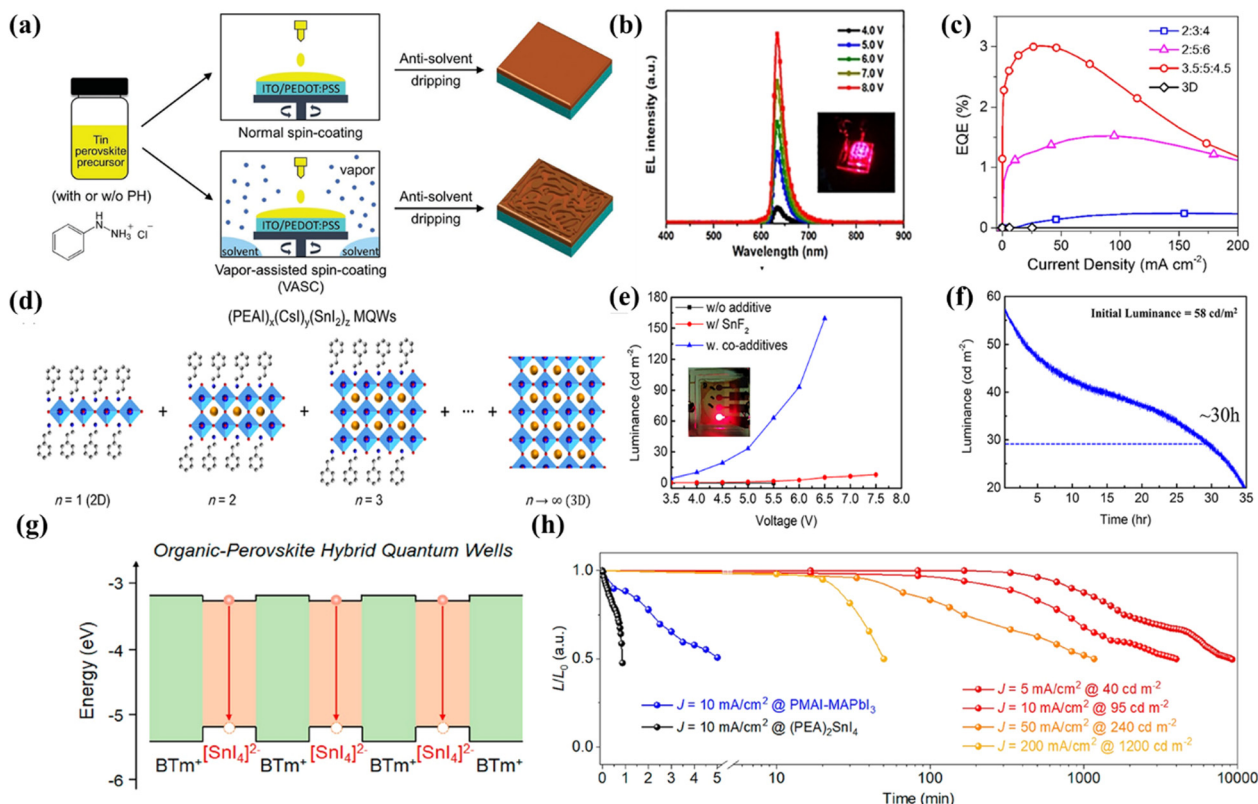
Fig. 1 (a) Fabrication procedure of PEA$_2$SnI$_4$ films by using an antisolvent-based normal spin-coating or vapor-assisted spin-coating (VASC) method. The VASC method is conducted by adding 200 μL of mixed solvent to the spin-coater to form solvent vapor before depositing perovskites. Copyright 2022, Wiley-VCH.[27] (b) Electroluminescent (EL) spectra of PEA$_2$SnI$_4$ LEDs. Reproduced with permission.[18] (c) EQE values *versus* current density. For the 3.5:5:4.5 MQW-based LEDs, a maximum EQE of 3% is achieved. Copyright 2019, American Chemical Society.[28] (d) Schematic of (PEAI)$_x$(CsI)$_y$(SnI$_2$)$_z$ perovskite MQWs composed of various perovskites with different inorganic layer numbers (*n*). Copyright 2019, American Chemical Society.[28] (e) Luminance–voltage. The LEDs with SnF$_2$: TPBI co additive are 13 times brighter than LEDs with SnF$_2$ only (*L* ≈ 107 cd m^{-2}). Copyright 2022, American Chemical Society.[29] (f) Operational lifetime of CsSnBr$_3$ LEDs. Copyright 2022, American Chemical Society.[29] (g) Schematic of relative band alignment of organic (BTm$^+$) and inorganic ([SnI$_4$]$^{2-}$) layers within 2D hybrid perovskites. The red arrows indicate the radiative recombination of confined excitons in such 2D HQWs. Copyright 2021, American Chemical Society.[30] (h) Operational lifetime of the hybrid perovskite LEDs devices for (PEA)$_2$SnI$_4$ (black), PMAI-MAPbI$_3$ (blue), and (BTm)$_2$SnI$_4$ at different current densities (from yellow, orange, and red to dark red). These unencapsulated devices were tested in a glovebox with constant driving current densities. Copyright 2021, American Chemical Society.[30]

photograph of the fabricated electrically driven blue LEDs with a size of 1 mm^2, showing current-density–luminance–voltage (*J–L–V*) characteristics. Unfortunately, the EL characteristics are still insufficient compared with the those of traditional CsPbX$_3$ based LEDs;[35] the main reason for the low device efficiency is that the Cs$_3$Cu$_2$I$_5$ film prepared by solution technology has a poor morphology. Later, Wu *et al.* prepared a continuous and pin-hole-free Cs$_3$Cu$_2$I$_5$ thin film by a double source thermal evaporation method for the first time (Fig. 2d and e) with a PLQY of 58%.[36] Shan *et al.* successfully prepared electrically driven dark blue LEDs with Cs$_3$Cu$_2$I$_5$ nanocrystals (NCs) and obtained EQE up to 1.12%. Fig. 2b shows the EL spectra of LEDs under different voltages. A bright blue emission is observed at 445 nm, which matches well with the PL spectrum of Cs$_3$Cu$_2$I$_5$ NCs. With the increase of bias voltage, the emission intensity increases monotonously and the peak position remains unchanged, which is comparable to the blue LEDs based on lead(II) halide perovskite with the best performance.[37] The introduction of additives facilitates holes to repair and

controls the rate of crystal growth. Thereafter, Liu and coworkers prepared Cs$_3$Cu$_2$I$_5$ nanocrystals using an improved thermal injection strategy by using InI$_3$ as the precursor. The single-phase nanocrystal has a bright dark blue emission peaked at 440 nm. When the content of InI$_3$ reaches 0.15 mmol, its PLQY reaches a record value of 96.6%. Then they prepared a Cs$_3$Cu$_2$I$_5$ NCs solid film on the SiO$_2$/Si substrate using a spin-coating method. The as-fabricated devices exhibited a half-lifetime of more than 300 hours under a driving current of 10 mA, which is comparable to that of the most advanced lead(II)-based perovskite LED device.[38]

In addition to the dark blue PeLEDs of Cs$_3$Cu$_2$I$_5$ summarized above, CsCu$_2$I$_3$ is another ternary copper halide developed intensively, which exhibits yellow emission. Shi *et al.* first proved that ternary copper halide Cs$_3$Cu$_2$I$_5$ nanocrystals (NCs) have excellent hydrochromic properties. The NC film can realize reversible conversion between blue-emitting (445 nm) Cs$_3$Cu$_2$I$_5$ and yellow-emitting (567 nm) CsCu$_2$I$_3$ by exposing to/removing water. This new discovery has deepened the understanding of
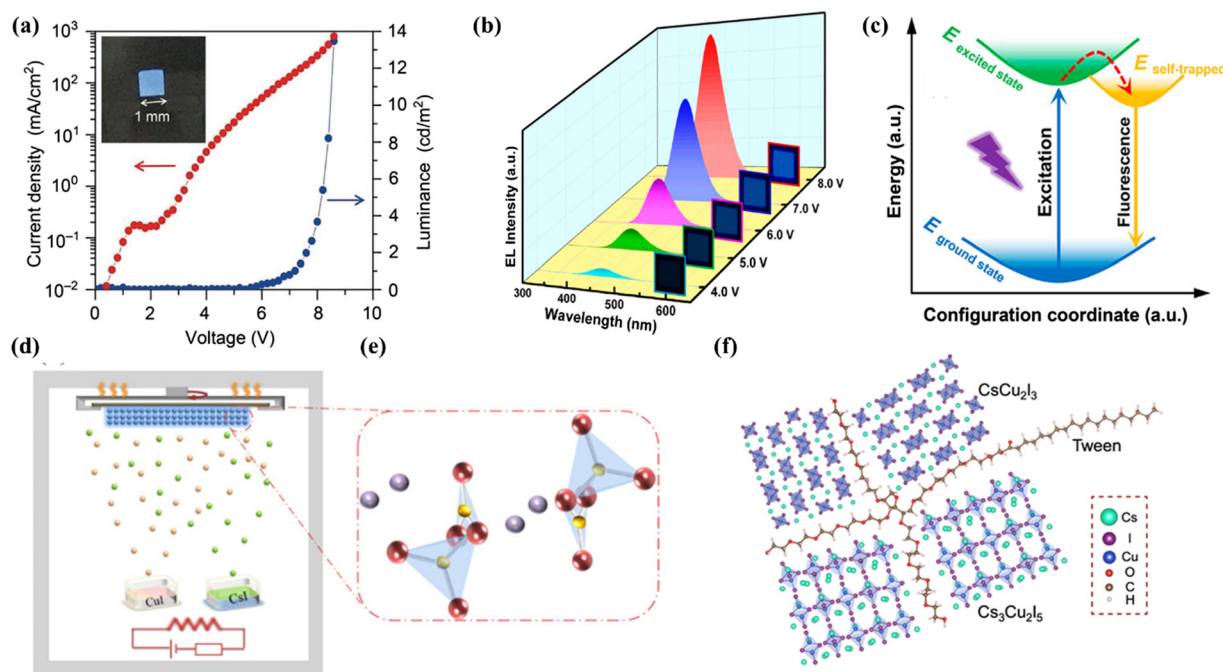
Fig. 2 (a) Current-density–luminance–voltage characteristic curve of the blue LEDs using a $Cs_3Cu_2I_5$ thin film as an emission layer, and its photograph (inset). Copyright 2018, Wiley-VCH.[36] (b) EL spectra of the $Cs_3Cu_2I_5$ NCs LEDs at different applied voltages. Copyright 2020, American Chemical Society.[38] (c) Configuration coordinate diagram for the STEs dynamic mechanism of the $CsCu_2I_3$ thin films. Copyright 2020, American Chemical Society.[41] (d) Illustration of film deposition by dual-source thermal evaporation of $Cs_3Cu_2I_5$. (e) Crystal structure of $Cs_3Cu_2I_5$. Copyright 2020, American Chemical Society.[37] (f) Characterization of cesium–copper–iodide films with Tween. Copyright 2021, Springer Communications.[42]

$Cs_3Cu_2I_5$ and $CsCu_2I_3$,[39] where 1D $CsCu_2I_3$ has a FWHM (full width at half maximum) of 107 nm which is wider than that of $Cs_3Cu_2I_5$. Ma *et al.* pointed out that the yellow LEDs prepared using $CsCu_2I_3$ have good color stability and low toxicity. Fig. 2c shows the STE dynamics mechanism of the $CsCu_2I_3$ film. The maximum brightness of the device is 47.5 cd m^{-2}, the EQE is 0.17%, and the half-lifetime at 25 °C is 5.2 h, while the device can still work normally at 60 °C with a half-lifetime of 2.2 h.[40]

Later, Shan's team reported $CsCu_2I_3$ thin films prepared by a one-step spin-coating method with PVK (9-vinylcarbazole) additives of different concentrations in the precursor solutions, and eco-friendly and stable yellow LEDs devices were obtained. Doping PVK with a carbazole group into the $CsCu_2I_3$ emitter can inhibit anti-site defects and enhance radiation recombination. The peak EQE of the polymer PVK modified LEDs is 1.35%, which is about 8.5 times that of the original device (0.16%).[42] Similar to the preparation processes of $Cs_3Cu_2I_5$ thin films, the morphology of the $CsCu_2I_3$ thin films can also be improved by choosing appropriate process methods. Thus, the performance of electrically driven LEDs can be further optimized.

Tang and co-workers prepared a $CsCu_2I_3$ layer by the vacuum deposition method and obtained yellow emitting LEDs.[43] The device adopted the optimized ITO/NiOx/$CsCu_2I_3$/TPBi/LiF/Al structure with a luminous brightness of 10 cd m^{-2} and an EQE of 0.02%. Thereafter, Kim *et al.* successfully used the VTE co-evaporation film deposition process to prepare the $CsCu_2I_3$ emission layer. The PLQY was significantly increased

to 84.8%, and the EQE boosted to 7.4%, representing the state-of-the-art for Cu(I) based PeLEDs.[44] The complementary colors originated from $CsCu_2I_3$ and $Cs_3Cu_2I_5$ can cover almost the entire visible spectral region and thus these compounds exhibit white emission. Based on this, Wang's group demonstrated efficient and bright LEDs based on $CsCu_2I_3@Cs_3Cu_2I_5$ enabled by introducing an organic additive (Tween) into the precursor solutions. Fig. 2f shows the structural diagram of the mixture of $Cs_3Cu_2I_5$ and $CsCu_2I_3$ microcrystals. It is found that the additive can reduce the trap states, enhance the PLQY, and increase the surface potential, thus facilitating the hole injection and transport in the LEDs. Consequently, warm-white LEDs with an EQE of 3.1% and a luminance of 1570 cd m^{-2} at a low voltage of 5.4 V were obtained, showing great potential of lead-free metal halides for solution-processed white LED applications.[41]

Shan's team adopted a simple one-step method to synthesize a $CsCu_2I_3@Cs_3Cu_2I_5$ composite. The composite material showed perfect white light emission, cold/warm white light tuning and strong stability against heat, ultraviolet light and environmental oxygen/water. Subsequently, a series of cold/temperature adjustable white light-emitting diodes (WLEDs) were prepared, where the maximum brightness of 145 cd m^{-2}, an EQE of 0.15%, and a CRI of 91.6 were achieved, which is the highest value among those of lead-free WLEDs.[45] In addition to the all-inorganic copper halides, copper-based organic–inorganic hybrid materials also exhibit great potential for application in eco-friendly OLEDs. Li *et al.* investigated carrier transport of 2D CuI(L)$_{0.5}$ (L = organic ligand) single crystals,

obtaining a Hall mobility of 1 and 0.13 cm^2 V^{-1} S^{-1} for 2D CuI(pm)$_{0.5}$ and CuI(pz)$_{0.5}$, respectively, which are higher than those of typical light-emitting semiconductor materials.[46] Then they reported bright yellow PeLEDs based on a copper(I) iodide hybrid with the emission layer of 1D-Cu$_4$I$_6$(bttmp)$_2$ (bttmp = 3-(1*H*-benzo-[*d*][1,2,3]triazol-1-yl)-*N*,*N*,*N*-trimethylpropan-1-aminium). High quality 1D-Cu$_4$I$_6$(bttmp)$_2$ thin films with a PLQY of 91% were prepared by a simple one-step spin-coating process, and showed good stability in air and moisture and exceptional solution processability. The as-fabricated devices gave an EQE of 5.02% and a half-lifetime of 35.5 h under environmental conditions.[47]

4. Mn(II)-based electrically driven LEDs

Eco-friendly organic manganese(II) halide hybrids have been reported to exhibit strong photoluminescence (PL) with colours ranging from green to red. The luminescence mechanisms of this class of materials are also well known, that is, from the d–d transitions in tetrahedral and octahedral crystal fields for green and red emissions,[48] respectively. Due to high luminescence efficiency and good solution processability, our group attempted to fabricate the first solution-processed electrically driven LEDs based on Mn(II) hybrids in 2017 using 0D [PPh$_4$]$_2$[MnBr$_4$] as the light-emitting material.[20] The electroluminescence was identified to originate from the ^{4}T$_1$–^{6}A$_1$ transition of the Mn(II) ions with a tetrahedral coordination geometry, as revealed by the solid UV-vis absorption and emission spectral studies of [PPh$_4$]$_2$[MnBr$_4$] crystals. For the non-doped device, the peak current efficiency, power efficiency, and EQE are 25 cd A^{-1}, 18.3 lm W^{-1} and 7.2%, respectively. For the doped device, the device performance was distinctly improved with a peak current efficiency, a power efficiency and an EQE of 32.0 cd A^{-1}, 16.2 lm W^{-1} and 9.6% (Fig. 3a), respectively. Thereafter, Zhao and Huang *et al.* reported a new

type of neutral tetrahedral manganese(II) complexes for vacuum-deposited phosphorescent organic-light emitting diodes (PHOLEDs). The manganese (II) complexes (DBFDPO-MnBr$_2$) exhibit intense green phosphorescence with a PLQY of as high as 81.4%. Using complex DBFDPO-MnBr$_2$ as a green-emitting dopant, electrically driven LEDs (Fig. 3b) with a current efficiency of 35.47 cd A^{-1}, a power efficiency of 34.35 lm W^{-1} and an EQE of 10.49% were achieved. The EL spectra and the corresponding PL spectra of doped and undoped devices were studied as shown in Fig. 3c.[49] Hyunsik *et al.* fabricated highly efficient electrically driven LEDs using a zero-dimensional organic–inorganic hybrid [(H$_2$C = CHCH$_2$)(C$_6$H$_5$)$_3$P]$_2$MnBr$_4$. They achieved a highly efficient all-vacuum-deposited LEDs with a current efficiency of 24.71 cd A^{-1}, a power efficiency of 20.61 lm W^{-1}, and an EQE of 7.12%.[50] Besides, Yan *et al.* reported a 0D red-emitting hybrid (ABI)$_4$MnBr$_6$ (ABI, 2-aminobenzimidazole) with the emission peaked at 629 nm due to the octahedron coordination geometry and quantum yield of over 80%. The neat film of (ABI)$_4$MnBr$_6$ was used as the emitting layer for the fabrication of electrically driven LEDs. The maximum brightness and EQE were 4700 cd m^{-2} and 9.8%, respectively (Fig. 3d).[51] Fig. 3e shows the preparation process of (ABI)$_4$MnBr$_6$ crystals, in which A is the crystal morphology under environmental conditions, B is the crystal luminescence under 365 nm ultraviolet irradiation and C and D are crystal structure diagrams.

5. Sb(III)-based electrically driven LEDs

Antimony(III)-halides have been extensively explored due to their diverse topologies along with unique optical properties. Due to the diversity of topological structures and fascinating optical properties, they show broad application prospects in the field of optoelectronics. However, the attempt on the fabrication
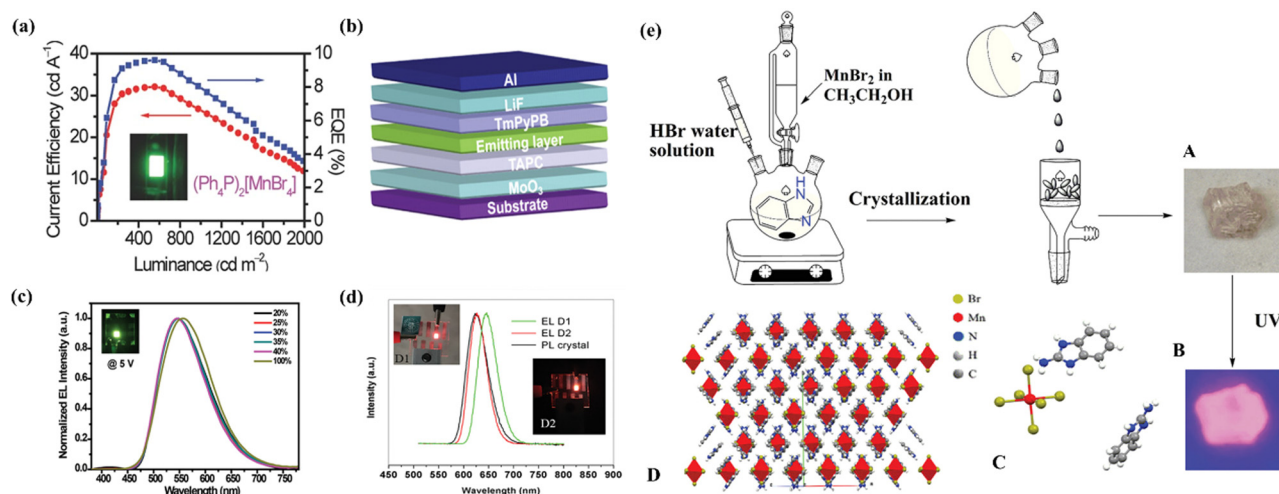
Fig. 3 (a) Current-density−EQE−luminance characteristics of the green LEDs using a (Ph$_4$P)$_2$[MnBr$_4$] thin film as the emission layer and its photograph (inset). Copyright 2016, Wiley-VCH.[20] (b) Structure of the DBFDPO-MnBr$_2$ device. Copyright 2018, Wiley-VCH.[49] (c) Normalized EL spectra of devices with different dopants. Copyright 2018, Wiley-VCH.[49] (d) EL spectrum of (ABI)$_4$MnBr$_6$ at 6 V. Inserted photographs show the devices at a voltage of 6.5 V. Copyright 2021, Wiley-VCH.[51] (e) The preparation of (ABI)$_4$MnBr$_6$ perovskite crystals. Copyright 2021, Wiley-VCH.[51]
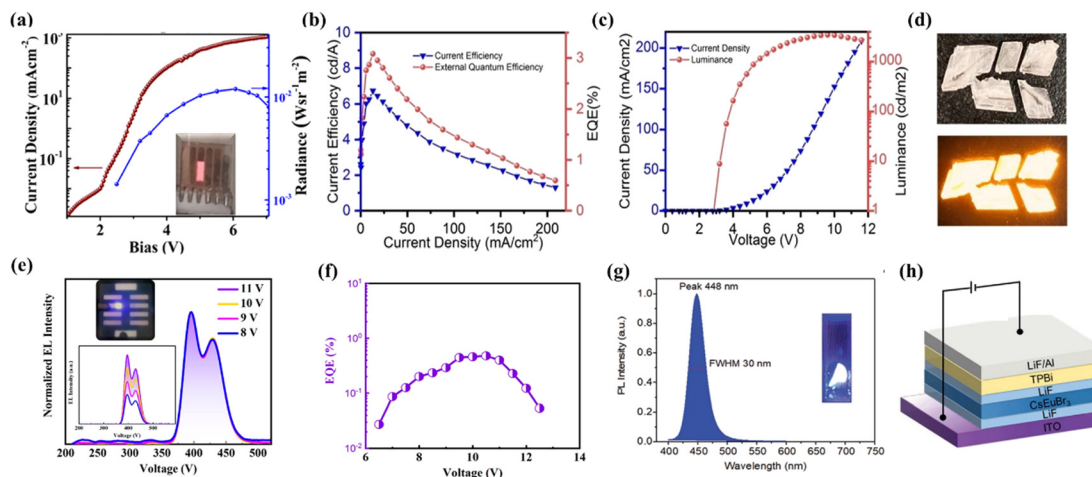
Fig. 4 (a) Current density *versus* voltage (*J*–*V*) and radiance *versus* voltage characteristics of $Cs_3Sb_2I_9$. Copyright 2019, American Chemical Society.[52] (b) The EQE/current efficiency *versus* current density for the doped device.[54] (c) The current density–voltage–luminance (*J*–*V*–*L*) characteristics of the doped device. Copyright 2022, Wiley-VCH.[54] (d) The images of $(MePPh_3)_2SbCl_5$ crystals under ambient light (up) and UV light (bottom) at 365 nm. Copyright 2022, Wiley-VCH.[54] (e) The normalized EL spectra of the Cs_3CeBr_6 LEDs at different applied voltages. The inset plot shows the photograph of a working violet light device and the EL spectra of the device operated at various voltages. Copyright 2021, American Chemical Society.[55] (f) The EQE– current density curve of Cs_3CeBr_6 LEDs. Copyright 2021, American Chemical Society.[55] (g) The PL spectrum of $CsEuBr_3$ crystals with 365 nm UV excitation at room temperature, and the inset shows the photograph of $CsEuBr_3$ under 365 nm UV light. Copyright 2022, Wiley-VCH.[56] (h). The device structure of $CsEuBr_3$ based LEDs. Copyright 2022, Wiley-VCH.[56]

of electrically driven LEDs is still in its infancy. Chu *et al.* synthesized all-inorganic antimony(III) based two-dimensional $Cs_3Sb_2I_9$ by a hot-injection method. The electrically driven LEDs were fabricated as shown in Fig. 4a, which exhibited a visible-infrared radiance of 0.012 W Sr^{-1} m^{-2} and a very low EQE of $\sim 10^{-8}$ when $Cs_3Sb_2I_9$ was employed as the active emitter layer.[52] Thereafter, Ma *et al.* fabricated electrically driven blue-emitting LEDs using lead-free $Cs_3Sb_2Br_9$ quantum dots, giving a purple emission (408 nm) at room temperature, which was the shortest wavelength reported at that time. The EQE of the device reached 0.206%. It is noteworthy that the device exhibited good device stability with only about 10% emission attenuation after six hours of continuous operation.[53] Recently, our group has successfully developed a 0D antimony halide hybrid $(MePPh_3)_2SbCl_5$, which shows strong orange emission (Fig. 4d) resulting from self-trapped exciton emission. Good stability, excellent solution processability and high PLQY make it suitable for electrically driven LEDs. Electrically driven LEDs based on neat and doped films of $(MePPh_3)_2SbCl_5$ were fabricated. The doped devices show a significant improvement in comparison to non-doped devices. Owing to the improved surface morphology and balanced carrier transport in the light-emitting layers of the doped devices, the peak luminance, current efficiency and EQE are boosted from 82 to 3500 cd m^{-2}, 1.1 to 6.8 cd A^{-1}, and 0.7% to 3.1% relative to those of non-doped devices, respectively (Fig. 4b and c).[54]

6. Lanthanide(III)-based electrically driven LEDs

Electrically driven LEDs based on lanthanides(III) have been also reported in recent years. The lanthanide(III) ions have similar ionic radii to that of Pb^{2+}. In addition, they also have

the advantages of high energy conversion efficiency, good stability, and emission wavelength in the dark blue to infrared region. Tang *et al.* prepared Cs_3CeBr_6 thin films based on thermal evaporation and fabricated the first electrically driven LEDs based on Cs_3CeBr_6. As shown in Fig. 4e, the EL spectrum of the device matched well with the PL spectrum of the Cs_3CeBr_6 film. The maximum EQE of the device is 0.46% (Fig. 4f), which is higher than those of the previously reported perovskite based purple LEDs.[55] In the same year, they reported a highly emissive $CsEuBr_3$, which exhibited bright blue exciton emission at 448 nm as depicted in Fig. 4g. Dark blue electrically driven LEDs (Fig. 4h) were prepared using a full vacuum deposition procedure with the maximum brightness of 5.2 cd m^{-2} and a peak EQE of 6.5%.[56]

7. Conclusion

We reviewed the development in the field of electrically driven LEDs based on lead-free metal halides including the synthesis of materials and the performance of devices from Sn(II) to Cu(I), Mn(II), Sb(III) and Ln(III) metal halides. The intriguing optical properties and device performances make this class of materials as potential candidates for the application in light-emitting displays and illumination devices. While remarkable progress has been achieved, many issues and challenges still need to be surmounted to achieve efficient and stable electrically driven LED devices. First, most of the hybrids exhibit high PLQY in crystalline states, but the emission intensity would experience a significant decrease in the film formation process due to the imperfect crystals of the precursors after solvent evaporation. Optimization of the film formation *via* component engineering, solvent engineering, dimensional control, and defect passivation

is an alternative method for enhancing the quality of films. Second, carrier mobility and conductivity of the metal halides reported so far are relatively low, which is not conducive to hole/electron migration from the transporting layer to light-emitting layer. The design and development of functional metal halides with better carrier mobility are urgently desirable for achieving highly efficient electrically driven LEDs. Third, the relationship between the emission details (mechanism, excited state character, *etc*.) and metal halides and the device efficiencies needs to be deeply established and understood, which will provide a good guideline for this class of materials toward achieving a high device performance. Besides, the device stability is still unsatisfied, great efforts are required to optimize the device fabrication process such as developing and adopting more suitable carrier transporting materials, and modifying the process of device encapsulation. Undoubtedly, the sustainable development of lead-free electrically driven LEDs will promote a new round of research and prosperity in the field of light-emitting materials and opto-electronic devices. With tremendous interest in this class of materials from both academic and industrial researchers, we expect more breakthroughs in this field in near future.

Conflicts of interest

There are no conflicts to declare.

Acknowledgements

Notes and references

1 C. W. Tang and S. A. VanSlyke, *Appl. Phys. Lett.*, 1987, **51**, 913–915.
2 F. So, J. Kido and P. Burrows, *MRS Bull.*, 2008, **33**, 663–669.
3 Y. Cao, N. Wang, H. Tian, J. Guo, Y. Wei, H. Chen, Y. Miao, W. Zou, K. Pan, Y. He, H. Cao, Y. Ke, M. Xu, Y. Wang, M. Yang, K. Du, Z. Fu, D. Kong, D. Dai, Y. Jin, G. Li, H. Li, Q. Peng, J. Wang and W. Huang, *Nature*, 2018, **562**, 249–253.
4 Y. X. Hu, J. Miao, T. Hua, Z. Huang, Y. Qi, Y. Zou, Y. Qiu, H. Xia, H. Liu, X. Cao and C. Yang, *Nat. Photonics*, 2022, **16**, 803–810.
5 D. Liu, X. Liu, Y. Gan, Z. Liu, G. Sun, C. Shen, X. Peng, W. Qiu, D. Li, Z. Zhou, Z. Li, H.-L. Yip and S.-J. Su, *ACS Energy Lett.*, 2022, **7**, 523–532.
6 J. S. Kim, J. M. Heo, G. S. Park, S. J. Woo, C. Cho, H. J. Yun, D. H. Kim, J. Park, S. C. Lee, S. H. Park, E. Yoon, N. C. Greenham and T. W. Lee, *Nature*, 2022, **611**, 688–694.
7 C. Y. Kuei, W. L. Tsai, B. Tong, M. Jiao, W. K. Lee, Y. Chi, C. C. Wu, S. H. Liu, G. H. Lee and P. T. Chou, *Adv. Mater.*, 2016, **28**, 2795–2800.
8 Q.-C. Zhang, H. Xiao, X. Zhang, L.-J. Xu and Z.-N. Chen, *Coord. Chem. Rev.*, 2019, **378**, 121–133.
9 Z. K. Tan, R. S. Moghaddam, M. L. Lai, P. Docampo, R. Higler, F. Deschler, M. Price, A. Sadhanala, L. M. Pazos, D. Credgington, F. Hanusch, T. Bein, H. J. Snaith and R. H. Friend, *Nat. Nanotechnol.*, 2014, **9**, 687–692.
10 H. C. Cho, S.-H. Jeong, M.-H. Park, Y.-H. Kim, C. Wolf, S. H. Im, R. H. Friend and T.-W. Lee, *Science*, 2015, **350**, 6265.
11 Y. K. Wang, K. Singh, J. Y. Li, Y. Dong, X. Q. Wang, J. M. Pina, Y. J. Yu, R. Sabatini, Y. Liu, D. Ma, J. Liu, Z. Liu, Y. Gao, O. Voznyy,

12 W. Ma, M. K. Fung, L. S. Liao and E. H. Sargent, *Adv. Mater.*, 2022, **34**, 2200854.
12 Z. Liu, W. Qiu, X. Peng, G. Sun, X. Liu, D. Liu, Z. Li, F. He, C. Shen, Q. Gu, F. Ma, H. L. Yip, L. Hou, Z. Qi and S. J. Su, *Adv. Mater.*, 2021, **33**, 2103268.
13 N. K. Tailor, S. Kar, P. Mishra, A. These, C. Kupfer, H. Hu, M. Awais, M. Saidaminov, M. I. Dar, C. Brabec and S. Satapathi, *ACS Mater. Lett.*, 2021, **3**, 1025–1080.
14 S. Z. Wang, J. T. Wang, Y. H. Lou, Y. H. Zhou and Z. K. Wang, *Adv. Mater. Interfaces*, 2022, **9**, 2200772.
15 L. Kong, X. Zhang, C. Zhang, L. Wang, S. Wang, F. Cao, D. Zhao, A. L. Rogach and X. Yang, *Adv. Mater.*, 2022, **34**, 05217.
16 C. Zhou, H. Lin, Q. He, L. Xu, M. Worku, M. Chaaban, S. Lee, X. Shi, M.-H. Du and B. Ma, *Mater. Sci. Eng., R*, 2019, **137**, 38–65.
17 G. Zhou, B. Su, J. Huang, Q. Zhang and Z. Xia, *Mater. Sci. Eng., R*, 2020, **141**, 100548.
18 F. L. Yuan, X. P. Zheng, A. Johnston, Y.-K. Wang, C. Zhou, Y. Dong, B. Chen, H. Chen, J. Z. Fan and E. H. Sargent, *Sci. Adv.*, 2020, **6**, eabb0253.
19 L. Lanzetta, J. M. Marin-Beloqui, I. Sanchez-Molina, D. Ding and S. A. Haque, *ACS Energy Lett.*, 2017, **2**, 1662–1668.
20 L. J. Xu, C. Z. Sun, H. Xiao, Y. Wu and Z. N. Chen, *Adv. Mater.*, 2017, **29**, 1605739.
21 H. Lin, C. Zhou, Y. Tian, T. Siegrist and B. Ma, *ACS Energy Lett.*, 2017, **3**, 54–62.
22 C. M. Li and Z. Xia, *Chem. Soc. Rev.*, 2021, **50**, 2626–2662.
23 M. H. Du, *J. Chem. Phys.*, 2019, **151**, 181101.
24 Q. Fan, G. V. Biesold-McGee, J. Ma, Q. Xu, S. Pan, J. Peng and Z. Lin, *Angew. Chem., Int. Ed.*, 2019, **59**, 1030–1046.
25 K. R. Hansen, C. E. McClure, D. Powell, H. C. Hsieh, L. Flannery, K. Garden, E. J. Miller, D. J. King, S. Sainio, D. Nordlund, J. S. Colton and L. Whittaker-Brooks, *Adv. Opt. Mater.*, 2022, **10**, 2102698.
26 H. Liang, F. Yuan, A. Johnston, C. Gao, H. Choubisa, Y. Gao, Y. K. Wang, L. K. Sagar, B. Sun, P. Li, G. Bappi, B. Chen, J. Li, Y. Wang, Y. Dong, D. Ma, Y. Gao, Y. Liu, M. Yuan, M. I. Saidaminov, S. Hoogland, Z. H. Lu and E. H. Sargent, *Adv. Sci.*, 2020, **7**, 1903213.
27 F. Zhang, H. Min, Y. Zhang, Z. Kuang, J. Wang, Z. Feng, K. Wen, L. Xu, C. Yang, H. Shi, C. Zhuo, N. Wang, J. Chang, W. Huang and J. Wang, *Adv. Mater.*, 2022, **34**, 2203180.
28 Y. Wang, R. Zou, J. Chang, Z. Fu, Y. Cao, L. Zhang, Y. Wei, D. Kong, W. Zou, K. Wen, N. Fan, N. Wang, W. Huang and J. Wang, *J. Phys. Chem. Lett.*, 2019, **10**, 453–459.
29 J.-M. Heo, H. Cho, S.-C. Lee, M.-H. Park, J. S. Kim, H. Kim, J. Park, Y.-H. Kim, H. J. Yun, E. Yoon, D.-H. Kim, S. Ahn, S.-J. Kwon, C.-Y. Park and T.-W. Lee, *ACS Energy Lett.*, 2022, **7**, 2807–2815.
30 K. Wang, L. Jin, Y. Gao, A. Liang, B. P. Finkenauer, W. Zhao, Z. Wei, C. Zhu, T. F. Guo, L. Huang and L. Dou, *ACS Nano*, 2021, **15**, 6316–6325.
31 Z. Wang, F. Wang, B. Zhao, S. Qu, T. Hayat, A. Alsaedi, L. Sui, K. Yuan, J. Zhang, Z. Wei and Z. Tan, *J. Phys. Chem. Lett.*, 2020, **11**, 1120–1127.
32 W. L. Hong, Y. C. Huang, C. Y. Chang, Z. C. Zhang, H. R. Tsai, N. Y. Chang and Y. C. Chao, *Adv. Mater.*, 2016, **28**, 8029–8036.
33 J. Lu, X. Guan, Y. Li, K. Lin, W. Feng, Y. Zhao, C. Yan, M. Li, Y. Shen, X. Qin and Z. Wei, *Adv. Mater.*, 2021, **33**, 2104414.
34 Z. Xing, Z. Zhou, G. Zhong, C. C. S. Chan, Y. Li, X. Zou, J. E. Halpert, H. Su and K. S. Wong, *Adv. Funct. Mater.*, 2022, **32**, 2207638.
35 T. Jun, K. Sim, S. Iimura, M. Sasase, H. Kamioka, J. Kim and H. Hosono, *Adv. Mater.*, 2018, **30**, 1804547.
36 X. Liu, Y. Yu, F. Yuan, C. Zhao, H. Dong, B. Jiao and Z. Wu, *ACS Appl. Mater. Interfaces*, 2020, **12**, 52967–52975.
37 L. Wang, Z. Shi, Z. Ma, D. Yang, F. Zhang, X. Ji, M. Wang, X. Chen, G. Na, S. Chen, D. Wu, Y. Zhang, X. Li, L. Zhang and C. Shan, *Nano Lett.*, 2020, **20**, 3568–3576.
38 F. Gao, X. Zhu, C. Feng, W. Zhong, W. Liu, H. Xu and Y. Liu, *Nano Energy*, 2022, **98**, 107270.
39 F. Zhang, W. Liang, L. Wang, Z. Ma, X. Ji, M. Wang, Y. Wang, X. Chen, D. Wu, X. Li, Y. Zhang, C. Shan and Z. Shi, *Adv. Funct. Mater.*, 2021, **31**, 2105771.
40 Z. Ma, Z. Shi, C. Qin, M. Cui, D. Yang, X. Wang, L. Wang, X. Ji, X. Chen, J. Sun, D. Wu, Y. Zhang, X. J. Li, L. Zhang and C. Shan, *ACS Nano*, 2020, **14**, 4475–4486.
41 H. Chen, L. Zhu, C. Xue, P. Liu, X. Du, K. Wen, H. Zhang, L. Xu, C. Xiang, C. Lin, M. Qin, J. Zhang, T. Jiang, C. Yi, L. Cheng,

C. Zhang, P. Yang, M. Niu, W. Xu, J. Lai, Y. Cao, J. Chang, H. Tian, Y. Jin, X. Lu, L. Jiang, N. Wang, W. Huang and J. Wang, *Nat. Commun.*, 2021, **12**, 1421.

42 Z. Ma, X. Ji, M. Wang, F. Zhang, Z. Liu, D. Yang, M. Jia, X. Chen, D. Wu, Y. Zhang, X. Li, Z. Shi and C. Shan, *Adv. Sci.*, 2022, **9**, 2202408.

43 N. Liu, X. Zhao, M. Xia, G. Niu, Q. Guo, L. Gao and J. Tang, *J. Semicond.*, 2020, **41**, 052204.

44 G. Seo, H. Jung, T. D. Creason, V. Yeddu, M. Bamidele, E. Echeverria, J. Lee, D. McIlroy, B. Saparov and D. Y. Kim, *ACS Energy Lett.*, 2021, **6**, 2584–2593.

45 Z. Ma, Z. Shi, D. Yang, Y. Li, F. Zhang, L. Wang, X. Chen, D. Wu, Y. Tian, Y. Zhang, L. Zhang, X. Li and C. Shan, *Adv. Mater.*, 2021, **33**, 2001367.

46 W. Ki, X. Hei, H. T. Yi, W. Liu, S. J. Teat, M. Li, Y. Fang, V. Podzorov, E. Garfunkel and J. Li, *Chem. Mater.*, 2021, **33**, 5317–5325.

47 K. Zhu, Z. Cheng, S. Rangan, M. Cotlet, J. Du, L. Kasaei, S. J. Teat, W. Liu, Y. Chen, L. C. Feldman, D. M. O'Carroll and J. Li, *ACS Energy Lett.*, 2021, **6**, 2565–2574.

48 Y. Wu, X. Zhang, Y. Q. Zhang, M. Yang and Z. N. Chen, *Chem. Commun.*, 2018, **54**, 13961–13964.

49 Y. Qin, P. Tao, L. Gao, P. She, S. Liu, X. Li, F. Li, H. Wang, Q. Zhao, Y. Miao and W. Huang, *Adv. Opt. Mater.*, 2019, **7**, 1801160.

50 A. Jana, V. G. Sree, Q. Ba, S. C. Cho, S. U. Lee, S. Cho, Y. Jo, A. Meena, H. Kim and H. Im, *J. Mater. Chem. C*, 2021, **9**, 11314–11323.

51 S. Yan, W. Tian, H. Chen, K. Tang, T. Lin, G. Zhong, L. Qiu, X. Pan and W. Wang, *Adv. Funct. Mater.*, 2021, **31**, 2100855.

52 A. Singh, N. C. Chiu, K. M. Boopathi, Y. J. Lu, A. Mohapatra, G. Li, Y. F. Chen, T. F. Guo and C. W. Chu, *ACS Appl. Mater. Interfaces*, 2019, **11**, 35088–35094.

53 Z. Ma, Z. Shi, D. Yang, F. Zhang, S. Li, L. Wang, D. Wu, Y. Zhang, G. Na, L. Zhang, X. Li, Y. Zhang and C. Shan, *ACS Energy Lett.*, 2019, **5**, 385–394.

54 J. L. Li, Y. F. Sang, L. J. Xu, H. Y. Lu, J. Y. Wang and Z. N. Chen, *Angew. Chem., Int. Ed.*, 2022, **61**, 202113450.

55 L. Wang, Q. Guo, J. Duan, W. Xie, G. Ji, S. Li, C. Chen, J. Li, L. Yang, Z. Tan, L. Xu, Z. Xiao, J. Luo and J. Tang, *ACS Energy Lett.*, 2021, **6**, 4245–4254.

56 J. Luo, L. Yang, Z. Tan, W. Xie, Q. Sun, J. Li, P. Du, Q. Xiao, L. Wang, X. Zhao, G. Niu, L. Gao, S. Jin and J. Tang, *Adv. Mater.*, 2021, **33**, 2101903.